Exceptionally Strong Effect of Small Structural Variations in Functionalized 3,4-Phenylenedioxythiophenes on the Surface Nanostructure and Parahydrophobic Properties of Their Electropolymerized Films

Thierry Darmanin,*[,a] Elena L. Klimareva,[b,c] Irina Schewtschenko,[b] Frédéric Guittard,[a] and Igor F. Perepichka*[,d,b]

Abstract

Electropolymerization of electron-rich aromatics/heteroaromatics to form conducting polymers is an easy and powerful technique to form surfaces of different nanostructures and hydrophobicity/wettability. Understanding the factors governing the growth of the polymer nanostructures and controlling the surface morphology are the big challenges for the surface and materials science. In this paper we report design and synthesis of a series of 3,4-phenylenedioxythiophenes substituted at the benzene ring with 2-naphtylmethyl-, 1-naphtylmethyl-, and 9-anthracenylmethyl-groups (**2Na-PheDOT**, **1Na-PheDOT** and **9Ant-PheDOT**). They have been electropolymerized in either potentiostatic or potentiodynamic conditions to form the polymer surfaces of different morphologies. Even small changes in the structure of **PheDOT** monomers by varying the side groups (2-/1-naphtyl- or 9-anthracenyl-) result in formation of very different polymer surface nanostructures: from mono-directionally growing (1D) vertically aligned nanotubes for **2Na-PheDOT**, to ribbon-like nanostructures (2D) for **1Na-PheDOT**, and a mixture of these two structures for **9Ant-PheDOT**. Moreover, the surfaces of **p[2Na-PheDOT]** polymer, electrodeposited from the monomer **2Na-PheDOT** and the dimer **(2Na-PheDOT)$_2$** (which have different solubility and the reactivity on electropolymerization, but formally lead to the polymer of the same chemical structure) show very

[a] *Université Côte d'Azur, NICE Lab, IMREDD, 06200 Nice, France. Fax: (+33) 492076156. Tel.: (+33) 492076159. E-mail: thierry.darmanin@unice.fr*

[b] *School of Natural Sciences, Bangor University, Deiniol Road, Bangor LL57 2UW, UK. E-mail: i.perepichka@bangor.ac.uk*

[c] *Department of Organic Substances Technology, Ural Federal University, Ekaterinburg 620002, Russian Federation*

[d] *Shaanxi Institute of Flexible Electronics (SIFE), Northwestern Polytechnical University (NPU), 127 West Youyi Road, Xi'an 710072, P. R. China E-mail: i.perepichka@nwpu.edu.cn*

different nanostructures. In contrast to **2Na-PheDOT**, which forms vertically aligned nanotubes of the polymer on the surface, the polymerization of **(2Na-PheDOT)2** leads to spherical particles (3D) when Bu_4NClO_4 is used as an electrolyte and a membrane structure with spherical holes (3D) in the case of more hydrophobic Bu_4NPF_6. The importance of water for gas bubbles formation (O_2 and H_2) during electropolymerization and creation of the surface nanostructures has been demonstrated and discussed. The formation of these different nanostructures is accompanied by different wettability of the surface, from hydrophilic (with apparent water droplet contact angle of θ_w ~ 40 – 70 °) to highly hydrophobic (θ_w up to 129 – 134 °). Sticky, parahydrophobic surface formed from **1Na-PheDOT** showed high adhesion to water, with no water droplets move after inclination the surface to 90° (rose-petal effect).

Introduction

Controlling the surface nanostructure, hydrophobicity and water adhesion is very challenging task for various technological applications, including anti-fouling and self-cleaning surfaces,[1,2] water/fog harvesting,[3,4,5] microfluidic systems[6,7] and micropatterning.[8,9,10] Formation of such surfaces from conjugated polymers (CP) is of special interest because of simplicity of their preparation by electropolymerization of suitable aromatic/heteroaromatic monomers (e.g. based on functionalized thiophenes and pyrroles).[11,12,13] The other advantages are the formation of highly developed and/or ordered nanostructures without any surfactants or templates and wide range of possible shapes of surface nanostructures including nanotubes, nanocapsules, nanorings, nanosheets and nanobelts, as well as fibrous, sponge-like, tree-like, flower-like and cauliflower-like structures.[11,14,15,16,17,1819,20,21,22,23]

While intrinsically CP are generally hydrophilic, the formation of highly developed surfaces or porous structures during the electropolymerization may lead to parahydrophobic or superhydrophobic surfaces with extremely high water contact angles (θ_w) and high (for parahydrophobic) or low (for superhydrophobic) water adhesion.[24,25,26,27] The surface shape and the dimensions of the nanostructures, as well as the surface energy, hydrophobicity and water adhesion can be tailored by structural variations in used monomers, electrolytes and conditions of their electropolymerization in a controllable way.[16,28,29,30,31]

Polythiophenes are fascinating class of materials for organic electronics and optoelectronics.[32,33] Electropolymerization technique allows fast and easy deposition of electrically conducting polymer films using wide range of thiophene monomers (unsubstituted at positions 2,5). Poly(3,4-ethylenedioxythiophene) (**PEDOT**) is one of the mostly studied conducting polymers, with low oxidation potential, highly stable oxidized state and exceptional electronic properties.[34,35,36,37] Short

S···O contacts of neighboring **EDOT** moieties (confirmed by a single crystal X-ray diffraction for the oligomers) facilitate an improved rigidity and planarity of the polymer backbone contributing to its electronic properties.[38,39,40,41,42,43] Similar planarization of the backbone due to attractive S···O and Se···O interactions was also observed for some other related oligothiophenes/selenaphenes,[44,45,46,47,48] while its origin have not been fully understood and is a subject of current discussions.[49,50,51] Large number of **PEDOT** derivatives have been obtained by electrochemical or chemical polymerization of corresponding functionalized 3,4-ethylenedioxythiophene (**EDOT**) monomers and studied in a wide range of electronic and bioelectronic applications.[52,53,54] Different types of surfaces have also been reported for electrochemically deposited films of functionalized **PEDOTs**.[23,24,31,55,56,57,58]

3,4-Phenylenedioxythiophene (**PheDOT**),[59,60,61] a benzene-fused analog of **EDOT**, offer wider range of side-chain functionalization (alkyl or aryl substituents, electron-donating or electron-withdrawing groups at the benzene ring, Figure 1) expanding the library of monomers for conducting polymers.[59,60,62,63,64] Similar to **EDOT**, **PheDOT** can also be electropolymerized (at only slightly higher potential) to form the polymer, **p[PheDOT]**, with a planar structure of the main polymer chain.[61] The flat structure of **p[PheDOT]** itself and **p[PheDOT]s** substituted at the benzene ring have also been confirmed by DFT calculations.[63,64] A number of **PheDOT**-based polymers have been recently studied toward their self-assembly, electrochromic and photovoltaic properties.[62,65,66,67]

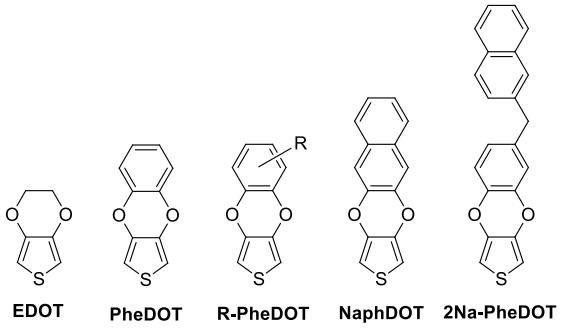


Figure 1. Structures of **EDOT**, **PheDOT** and functionalized **PheDOT**s.

Another exciting and unique property of functionalized **PheDOT** monomers is formation of rich variety of surface structures from electrodeposited polymers. Thus, we have recently demonstrated for the first time the formation of arrays of highly ordered, vertically aligned nanotubes by electropolymerization of 3,4-(1,2-naphtylene)dioxythiophene (**NaphDOT**)[68,69] and 3,4-(4-(2-naphtylmethyl)-1,2-phenylene)dioxythiophene (**2Na-PheDOT**) (Figure 1)[68,70] without any surfactant or template (templateless electropolymerization). Due to their structure, the electrodeposited polymers create highly hydrophobic surfaces with water contact angles up to θ_w = 135 ^{o} (Young's angle θ^Y =

63.6 °) and water droplets put on these substrates remain stuck even after inclination by 90 °.[68,69] Formation of other surface nanostructures from electropolymerized **PheDOT** derivatives including nanorings, sponge-like structures or vertically aligned nanofibers have also been recently demonstrated.[71,72] The nature of substituents at the benzene ring of **PheDOT** plays a crucial role in the polymers surface morphology. Thus, whereas in the case of polynuclear aromatic side moieties (as in the case of **NaphDOT** and **2Na-PheDOT**) nicely ordered nanotubes are created, for alkyl-substituted monomers **R-PheDOT** the tendency to form nanotubes and the roughness of the surface diminishes (from R = CH_3 to $C_{12}H_{25}$), although they also form surfaces with parahydrophobic properties ($\theta_w \approx 90 - 120$ °).[68] While for particular monomers, the surface nanostructures can be created in a controllable and reproducible way by proper choice of the conditions of electropolymerization, deeper understanding the relationships between the structure of the monomer and the structure of the resulting surfaces is still a challenging task.

Considering exceptional properties of the surface nanostructure of **p[2Na-PheDOT]** polymer obtained by electropolymerization of **2Na-PheDOT**,[68,70] in this work we have synthesized a series of related monomers with small variations in the side chain substituents (Figure 2). These included: (i) **1Na-PheDOT**, to look at the regio-isomerism effect (compared to **2Na-PheDOT**); (ii) **9Ant-PheDOT**, in which an additional benzene ring has been added at the side substituent; and (iii) oligomers **(2Na-PheDOT)$_2$** and **(2Na-PheDOT)$_3$**. In the last case, the electropolymerization should lead to the polymer **p[2Na-PheDOT]** of the same chemical structure as that from electropolymerization of the monomer **2Na-PheDOT.** On the other hand, it is known that the spin density on the terminal 2,5-thiophene carbon atoms in **PheDOT** oligomers is higher than that in the monomer and they are electropolymerized much faster and at lower concentrations than the **PheDOT** monomer.[61] Basing on that, we supposed that this might also effect on the morphology of the formed **p[2Na-PheDOT]** polymer films.

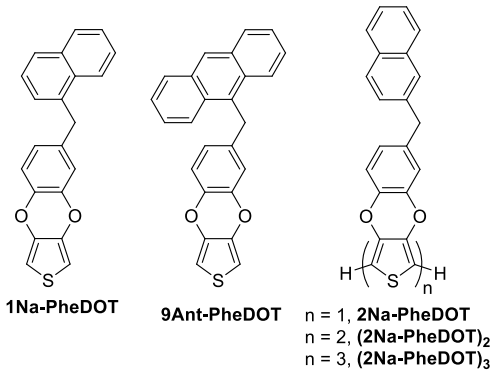
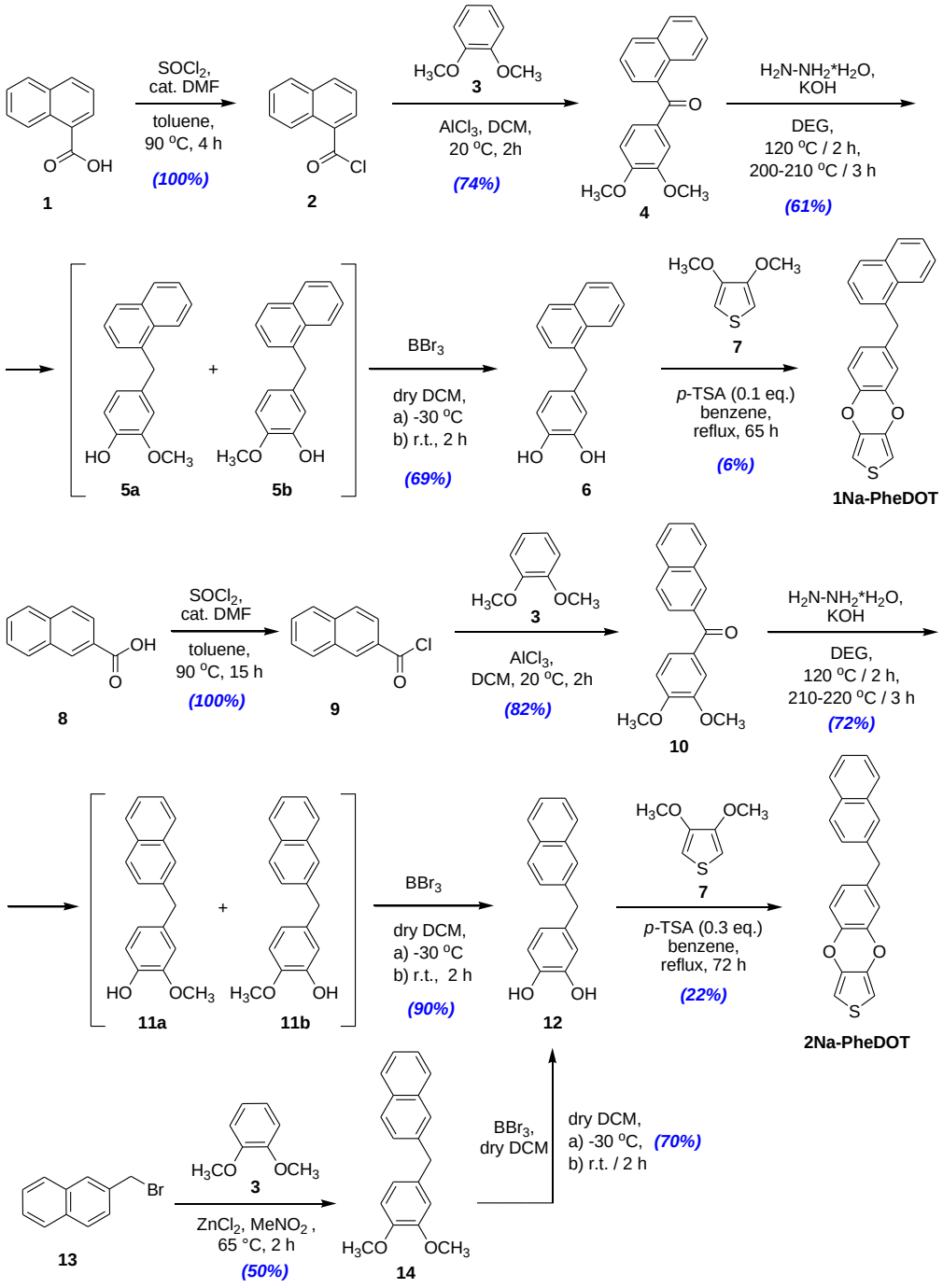


Figure 2. Structures of **1Na-PheDOT**, **9Ant-PheDOT** and **2Na-PheDOT** monomer, dimer and trimer.

Results and discussion

Synthesis and characterization of the monomers

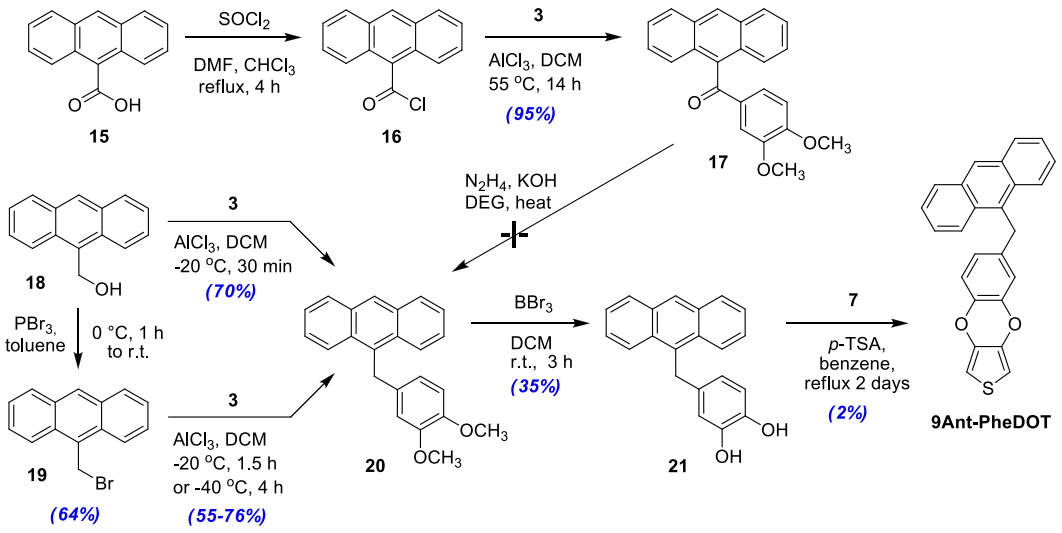
In synthesis of two isomeric naphtylmethyl-substituted 3,4-phenylenedioxythiophenes, **1Na-PheDOT** and **2Na-PheDOT**, we used the methodology described by us recently.[70] 1- and 2-Naphtoic acids (**1** and **8**) were converted to corresponding acyl chlorides **2** and **9**, respectively, which were then used in a Friedel-Crafts acylation of 1,2-dimethoxybenzene (**3**) to afford corresponding 4-naphtoyl-1,2-dimethoxybenzenes **4** and **10** in 74–82% yields, respectively (Scheme 1). The Wolff-Kishner reduction of the carbonyl group with hydrazine proceeded well, but in the alkali conditions of the reaction, one of the methoxy group was hydrolyzed resulting in a mixture of two regioisomers **5a,b** and **11a,b**, respectively, in approximately 1:1 ratio. This was not a problem as the target intermediates in the reaction schemes are catechols **6** and **12**, so no separation of the products "**a**" and "**b**" was required. These mixtures of two regioisomers (**5a,b** or **11a,b**) were used directly in the next step of demethylation with boron tribromide to remove methyl groups and afford catechols **6** or **12**, respectively. Catechol **12** was also obtained by Friedel-Crafts alkylation of 1,2-dimethoxybenzene (**3**) by 2-(bromomethyl)naphthalene (**13**) to afford compound **14**, following by its demethylation with BBr_3 (Scheme 1). The yield by this route was somewhat lower, but allowed quicker access to catechol **12** (2 steps instead of 4 steps starting from acid **8**). The obtained catechols **6** and **12** were then involved in the reaction with 3,4-dimethoxythiophene (**7**) under acidic catalysis with *p*-toluenesulfonic acid (*p*-TSA) (0.1–0.3 eq.) to afford two target monomers **1Na-PheDOT** and **2Na-PheDOT**, respectively. The **1Na-PheDOT** isomer was obtained with a low yield of 6% (comparable to 5% yield reported by us for **2Na-PheDOT**[70]), while the yield of **2Na-PhedOT** was improved to 22% when the reaction was performed in benzene (instead of toluene) with larger amount of *p*-TSA (0.3 eq.).



Scheme 1. Synthesis of **1Na-PheDOT** and **2Na-PheDOT**.

We tried to exploit the same synthetic route for synthesis anthracene derivative **9Ant-PheDOT** (Scheme 2). While intermediate **17** was obtained from acid **15** in near quantitative yield, its Wolff-Kishner reduction to **20** was unsuccessful giving a complex mixture of products, among which substantial amount of anthracene was identified. Therefore, intermediate **20** was obtained by Friedel-Crafts alkylation of 3,4-dimethoxybenzene (**3**) with anthracene-9-ylmethanol (**18**) or 9-

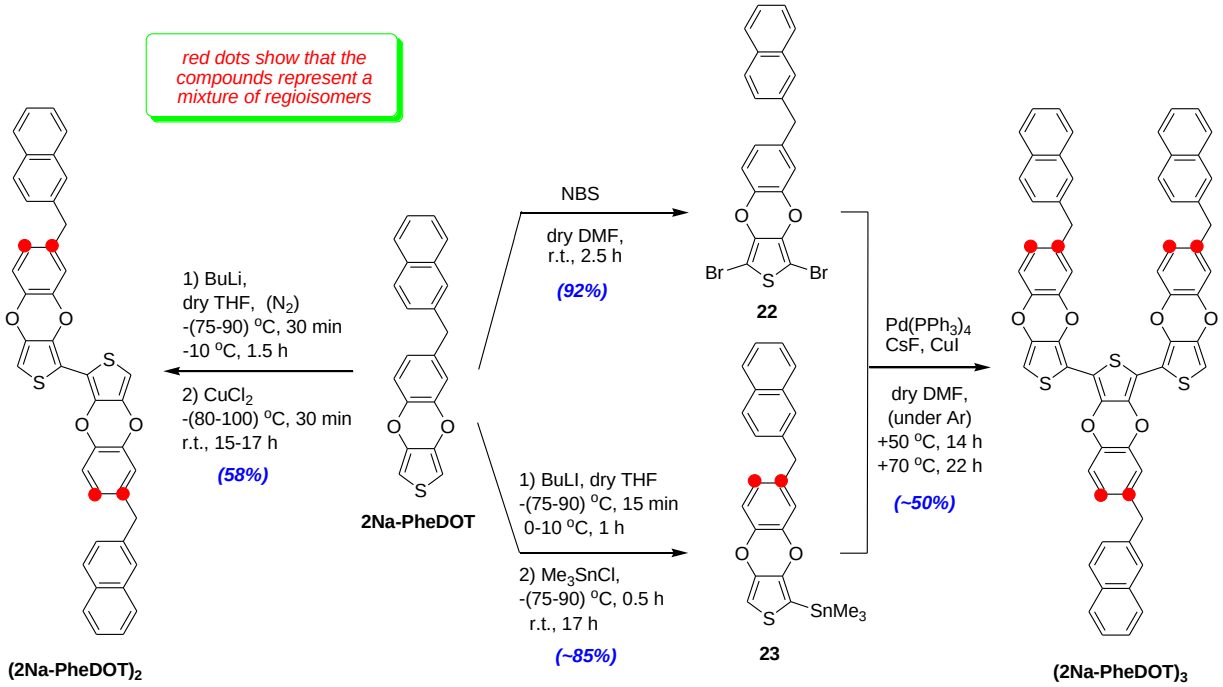
(bromomethyl)anthracene (**19**) affording the yields of 55 – 75%. It is critical to perform this reaction at very low temperature (–20 ~ –40 ^{o}C), because at temperatures >0 ^{o}C the cleavage of the product in acidic conditions was observed with formation of substantial amounts of anthracene (see experiments on p. S9 – S12 in the Supporting Information, SI). Low yield (35%) observed in the next step of demethylation of compound **20** with BBr_3 also confirms low stability of anthracene derivatives **20** and **21** in the presence of Lewis acids. The last step of acid-catalyzed condensation of catechol **21** with 3,4-dimethoxythiophene (**7**) was performed in conditions similar to synthesis of **1Na-PheDOT** and **2Na-PheDOT**. Target product **9Ant-PheDOT** was isolated with very low yield of ~2% and substantial amount of anthracene was formed in the reaction, which is in line with expected low stability of catechol **21** in acidic conditions.



Scheme 2. Synthesis of **9Ant-PheDOT**.

2Na-PheDOT monomer was used to prepare the dimer and trimer, **(2Na-PheDOT)$_2$** and **(2Na-PheDOT)$_3$** (Scheme 3). Lithiation of **2Na-PheDOT** with butyl lithium (BuLi) at low temperature, following the oxidative coupling of the lithiated intermediate with $CuCl_2$ resulted in the dimer **(2Na-PheDOT)$_2$** with 58% yield. As evidenced from ^{1}H NMR, the dimer was formed as a mixture of three regioisomers with different attachments of the 2-naphtylmethyl groups to the benzene rings, i.e. head-to-head, head-to tail and tail-to-tail (the positions are marked by red dots on Scheme 3). This is because the lithiation of **2Na-PheDOT** occurs at either position 2 or 5 of the thiophene ring. **2Na-PheDOT** was brominated with *N*-bromosuccinimide (NBS) in *N*,*N*-dimethylformamide (DMF) resulting in dibrominated product **22** with excellent yield of 92%. Lithiation of **2Na-PheDOT**, following by reaction of the lithiated intermediate with tributyltin chloride gave stannic derivative **23** as yellowish

oil with 96% yield (again, formed as a mixture of two regioisomers). According to ^{1}H NMR, the product's purity was around 85% (main by-product was starting of **2Na-PheDOT**) and it was used without further purification, because of its easy hydrolysis on flash chromatography on silica gel. Modified procedure of palladium-catalyzed Stille reactions in the presence of CuI and CsF[73] was used for coupling of dibromo- and tin-substituted compounds **22** and **23**, affording the trimer **(2Na-PheDOT)$_3$** within the yield of ~50%. The trimer **(2Na-PheDOT)$_3$** is a light-brown solid, insoluble in the most of the organic solvents (very low solubility in hot toluene or chlorobenzene). Its MALDI-TOF analysis coincides with the calculated mass-spectrum for the trimer (p. S64 in the SI). Due to apparently found very low solubility of the trimer **(2Na-PheDOT)$_3$** it was not used for electropolymerization and studies of the polymer surface.



Scheme 3. Synthesis of the dimer **(2Na-PheDOT)$_2$** and trimer **(2Na-PheDOT)$_3$**. The oligomers are obtained as a mixture of regioisomers (red dots show the positions of 2-naphtylmethyl group attachments).

Electropolymerization

The electropolymerization experiments were performed in dichloromethane (DCM) solutions with Bu_4NClO_4 as an electrolyte (0.1 M). For the monomers **2Na-PheDOT** and **1Na-PheDOT**, a typical concentration of 10 mM was selected. For the dimer **(2Na-PheDOT)$_2$**, we have initially used twice diluted concentration (5 mM), because of the presence of two **2Na-PheDOT** units in the structure. However, it was very difficult to dissolve the compound and it was also found that this concentration is

too high (so, the electrodeposition was too fast) for growing the nanoporous structures. Previously, we observed that electropolymerization of unsubstituted **PheDOT** dimer and trimer is much faster than that of the monomer.[61] Therefore, we chose a lower concentration of 0.5 mM for **(2Na-PheDOT)$_2$**.

After determination of their oxidation potentials (E^{ox} ≈ 1.67 – 1.80 V *vs.* SCE), the two monomers and the dimer were electropolymerized by cyclic voltammetry, cycling the potentials between –1 V and E^{ox} at a scan rate of 20 mV s^{-1} (Figure 3). The cyclic voltammograms showed the growth of the polymer films on the surface of the electrode as progressive currents at potentials lower than that for the monomers/dimer oxidation potentials. The intensities of the peaks of the polymer grown from the dimer **(2Na-PheDOT)$_2$** were higher than that from the monomers **1Na-PheDOT**, **2Na-PheDOT** and **9Ant-PheDOT** indicating on its faster electropolymerization (even at lower concentrations, 0.5 mM and 10 mM, respectively) and formation of thicker polymer films. Cyclic voltammograms of electrodeposited polymer films in a monomer-free solution showed electroactivity of doping/dedoping processes in the range of ≈ 0.70 – 1.1 V vs SCE, with onset oxidation potentials E_{pc}^{ox} ≈ 0.69 – 0.78 V (Figure S1 in the SI). These potentials are somewhat anodically shifted compared to **p[PheDOT]** films grown from unsubstituted **PheDOT** monomer,[59,61,63] due to the steric effects from bulky naphtylmethyl- and anthracenylmethyl- side groups, which prevents tight packing of the neighboring polymer chains.

It should be noted that electropolymerization of anthracene and naphthalene derivatives has also been described in the literature. However, in contrast to thiophene derivatives, which are readily electopolymerized, their electropolymerization generally proceeds efficiently in the media of high Lewis acidity (the Lewis acids forms π-complex with less reactive anthracene or naphthalene units to increase their ability for electropolymerization).[74,75,76,77] Therefore it is very unlikely that in the used conditions, naphthalene or anthracene moieties would be involved in and contribute to the electropolymerization process.

In the electropolymerization process, when traces of water are present in the system (from the solvent, salt or air atmosphere), formation of O_2 and H_2 gasses is possible within used range of scanned potentials. In anodic scans at positive potentials of ~1.5 – 2.0 V *vs.* SCE, an oxidation of traces of water can lead to formation of O_2 bubbles (eq. 1). This process is difficult to detect by cyclic voltammetry because the thiophene monomers (and the dimer) oxidation occurs at the same potentials (eq. 2). In cathodic scans at negative potentials of ca. –0.2 to –1.0 V, formation of H_2 bubbles can occur from the reduction of H^+ and traces of water in the solvent (eq. 3 and 4). It should be noted that in cyclic voltammetry electropolymerization, formation of H_2 gas bubbles (eq. 3) is possible not only from the reduction of H^+ generated from water oxidation (eq. 1), but also from the reduction of H^+ formed from

the monomer oxidative polymerization (eq. 2) (thus, 1 mol of the monomer can generate 1 mol of H_2). Such formation of O_2 and H_2 gasses as bubbles on the surface of formed polymer films is important for the formation of porous structures as they act as templates during the electropolymerization process.[68–70] These issues are discussed below.

$$2H_2O - 4e^- \rightarrow O_2\ (bubbles) + 4H^+ \quad (1)$$

$$n\cdot Monomer - 2ne^- \rightarrow Polymer + 2nH^+ \quad (2)$$

$$2H^+ + 2e^- \rightarrow H_2\ (bubbles) \quad (3)$$

$$2H_2O\ (traces) + 2e^- \rightarrow H_2\ (bubbles) + 2OH^- \quad (4)$$

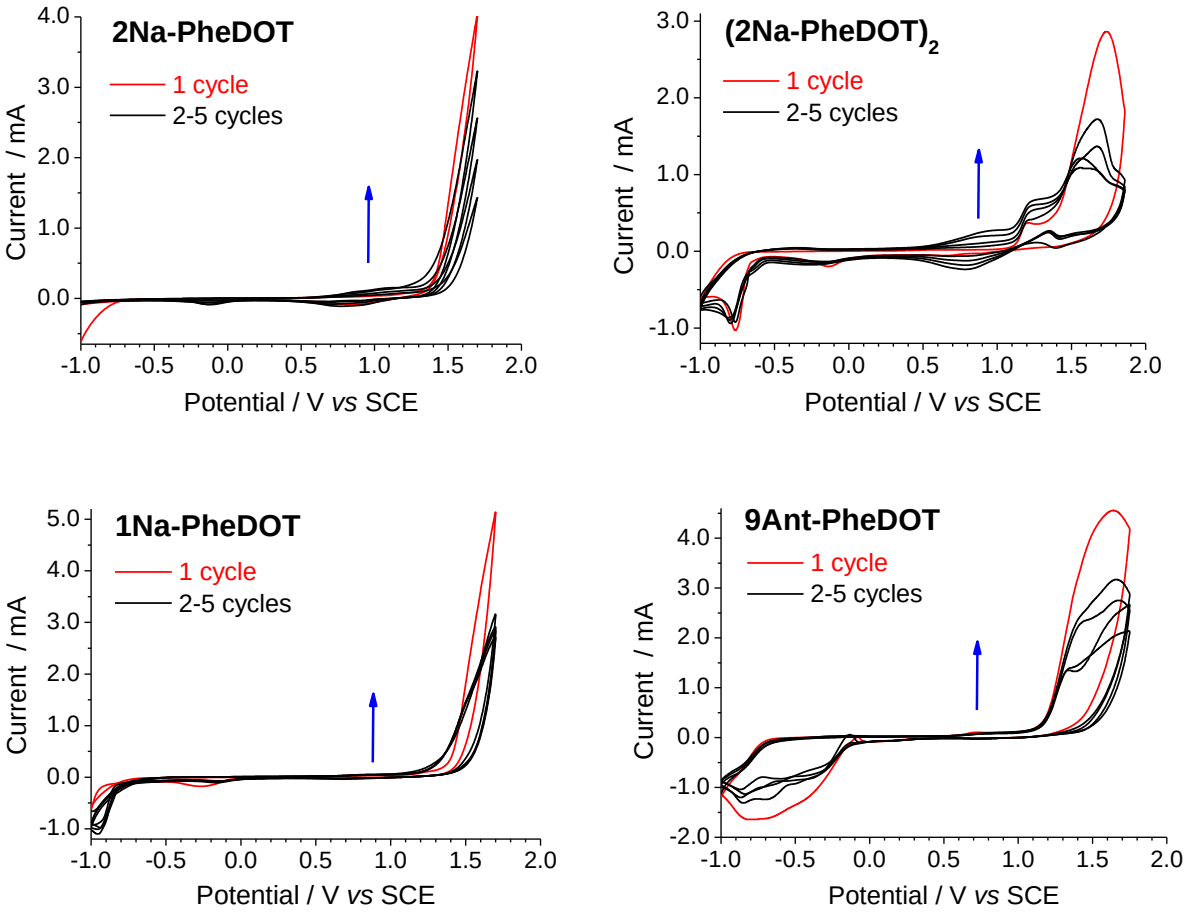


Figure 3. Electropolymerization of **2Na-PheDOT** (10 mM), **1Na-PheDOT** (10 mM) and **9Ant-PheDOT** monomers (10 mM), and **(2Na-PheDOT)$_2$** dimer (0.5 mM) by cyclic voltammetry in 0.1 M Bu_4NClO_4 / DCM at a scan rate 20 mV s^{-1}.

Surface morphology and nanostructures

Surfaces from potentiostatic polymerization. First, to investigate the growth of polymer films, the polymers were electrodeposited in 0.1 M Bu_4NClO_4 / DCM in potentiostatic conditions at constant potentials ($E^{ox} \approx 1.67 – 1.80$ V *vs.* SCE) using different deposition charges from 12.5 to 400 mC cm^{-2} (Figure 4, Figure 6 right column and Figures S3 – S13 in the SI). Analyzes of the polymer surfaces were also performed after the surface inclination by 45 ° in order to obtain a better view and an estimation of the dimensions of the nanostructures (Figure 5 and Figures S3, S4 and S10 – S13 in the SI). It should be mentioned that for deposition at constant potential of E^{ox}, only O_2 gas can be formed from traces of water (O_2 formation occurs at ≈ 1.5 – 2.0 V *vs.* SCE).

The SEM images demonstrated very significant changes in the surface morphology depending on the structure of the used monomers (Figure 4). All the monomers **2Na-PheDOT**, **1Na-PheDOT** and **9Ant-PheDOT** gave rise to nanotubules but the polymer films growth was clearly different. When using **2Na-PheDOT**, the vertically aligned nanotubes with diameters of ~100 nm were formed (Figure 4: **2Na-PheDOT**, 25 mC cm^{-2}), i.e. the growth was almost uniform and mono-directional (1D). When the deposition charge increased, this induced an increase of the height of the vertically aligned nanotubes and the size of the pores inside them, but the number of nanotubes having their opened tops decreased and at high deposition charge the tops of the nanotubes became to be closed (d ~ 300 – 500 nm; Figure 4: **2Na-PheDOT**, 100 – 200 mC cm^{-2}). In the case of **1Na-PheDOT**, the tubules grew in two directions (on elongation), but they were not vertically aligned leading to ribbon-like nanostructures (Figure 4, middle column and Figure S3 in the SI). Here, even if the growth is two-dimensional (2D) it is preferential in one of the two directions. This resulted in extremely long ribbon-like structures (up to 10 – 15 µm in length with ~ 300 – 800 nm in width) rather than square sheets. In the case of **9Ant-PheDOT**, densely packed interconnected nanocups with a near spherical shape and d ~ 150 – 500 nm were formed in the first instance (Figure 4, right column, 25 – 50 mC cm^{-2}). However, when the deposition charge increased, further polymer growth led to a mixture of nanotubes (as observed with **2Na-PheDOT**) and the nanoribbon-like structures (as with **1Na-PheDOT**), indicating that the growth of the nanostructures became more three-dimensional (3D) (Figure 4, right column (100 – 200 mC cm^{-2}) and Figures S6 – S13 in the SI).

The reactivity of the dimer **(2Na-PheDOT)$_2$** is much higher that that of the monomers.[61] Therefore, to adjust its electropolymerization rate to be comparable with the monomers, we used lower concentration (0.5 mM instead of 10 mM used for other monomers). In the case of the dimer **(2Na-PheDOT)$_2$**, only very small separate nanocups (d ~ 200 – 300 nm) were observed at low deposition charge leading to hollow nanospheres when the deposition charge increases (Figure 6, right column and

Figures S4 and S5 in the SI). When the deposition charge increased over 50 mC cm^{-2} and the porous structures were closed to form agglomerates, further growth became only 3D with formation of spherical nanoparticles on the surface. In order to understand better the observed results, it is important to cite the work of Wang et al.[78] They studied the formation of various nanostructures using aniline oligomers (trimers) formed in the first stage of aniline oxidation (another monomer often studied in the literature). The asymmetry of this molecule was found to be responsible for the formation of various assemblies such as nanofibers (1D-growth), nanosheets (2D-growth) or flower-like and urchin-like structures (3D-growth), depending on the experimental conditions (acidity, reaction time etc.). In our work, the experimental conditions were comparable and the different polymer surface nanostructures were governed by the substituents in the side chain of the monomers. Arylmethyl-groups in substituted **PheDOTs** are partly flexible, rotating and adopting minimum energy conformations in which the aromatic moieties are out-of-plane of the **PheDOT** unit (Figure S2 in the SI). Similar to **PEDOT**, the backbone of **p[PheDOT]** polymers is planar[59,61,62,64] that should favor the growth of flat polymer with strong π-stacking interactions between the neighboring chains. Bulky side groups can sterically effect on the degree of these interactions (and, possibly, on some distortion of the polymer backbone in the solid state). According to DFT calculations, the lowest steric hindrances should be observed for **2Na-PheDOT** (Figure S2 in the SI), for which the nanostructure growth occurs only in one direction. The structure of growing polymer is further slightly perturbed in the case of **1Na-PheDOT** and even more perturbed for **9Ant-PheDOT** with bulky anthracene side group, leading to changes from 1D nanotubes growth to 2D/3D ribbon-like structures. For the dimer **(2Na-PheDOT)$_2$**, which is much more reactive, the growth of the polymer surface is 3D because this molecule is very badly soluble and electropolymerizes faster (even at substantially lower concentrations), whereas the unidirectional 1D growth requires better soluble monomer/oligomer and longer time for adopting the shape of growing polymer chain.

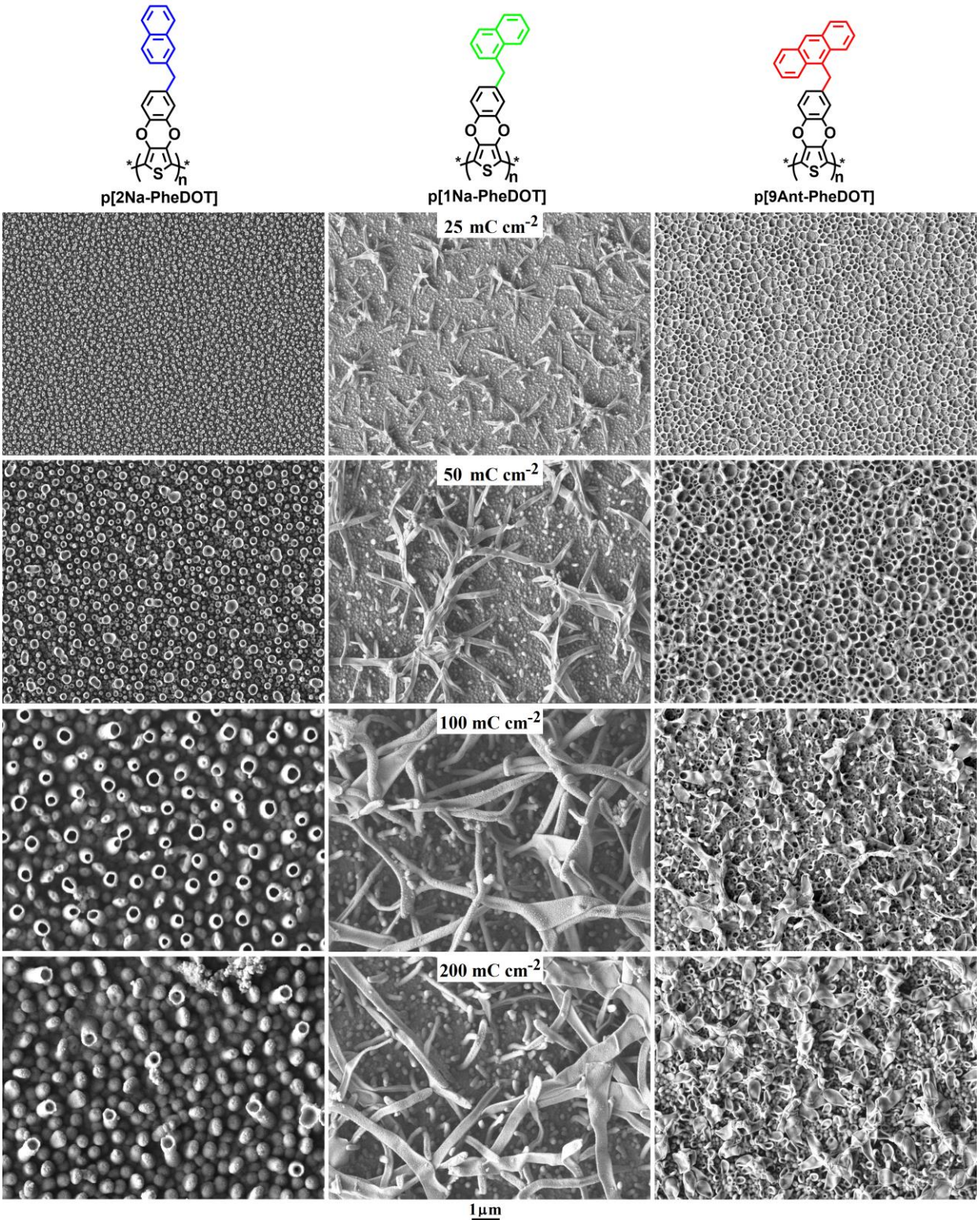


Figure 4. SEM images of the polymer surfaces electrodeposited from the monomers **2Na-PheDOT**, **1Na-PheDOT** and **9Ant-PheDOT** (10 mM) in 0.1 M Bu_4NClO_4 / DCM in potentiostatic conditions at constant potential of $E^{ox} \approx 1.70 - 1.80$ V *vs.* SCE and the deposition charges (from top to bottom) of Q_s = 25, 50, 100 and 200 mC cm^{-2}. Magnification: ×10,000.

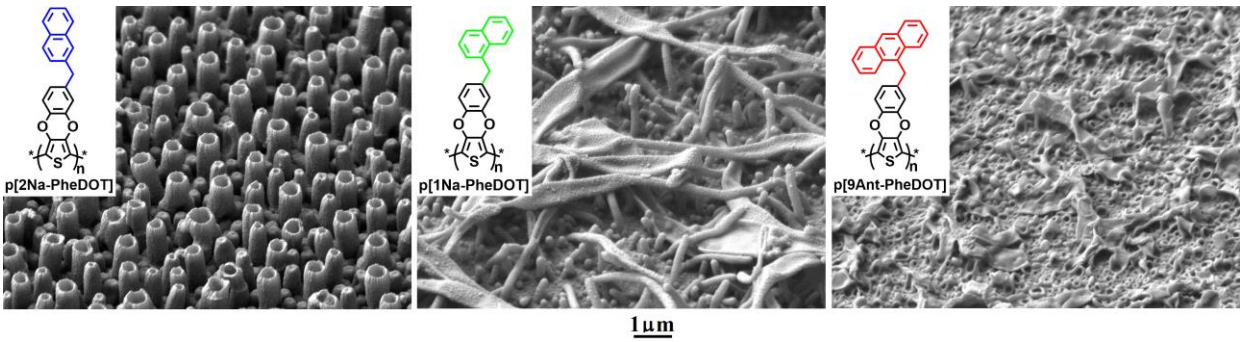


Figure 5. SEM images of the polymer surfaces electrodeposited from the monomers **2Na-PheDOT**, **1Na-PheDOT** and **9Ant-PheDOT** (10 mM) in 0.1 M Bu_4NClO_4 / DCM in potentiostatic conditions at constant potential of $E^{ox} \approx 1.70 - 1.80$ V *vs.* SCE and the deposition charges of $Q_c = 100$ mC cm^{-2}. Substrate inclination: 45 °; magnification: ×10,000.

Surfaces from potentiodynamic polymerization. We also electrodeposited the polymer films from the monomers **2Na-PheDOT**, **1Na-PheDOT** and **9Ant-PheDOT**, and the dimer **(2Na-PheDOT)$_2$** by cyclic voltammetry at a scan rate of 20 mV s^{-1} using different number of scans (1, 3 or 5). It should be mentioned that for potentiodynamic deposition by cyclic voltammetry within the used potential range, two kinds of gases can be formed from water (O_2 at ≈ 1.5 – 2.0 V and H_2 at ≈ –0.2 ~ –1.0 V *vs.* SCE). After electrodeposition of the polymer films, their surfaces were studied by SEM (Figure 6, left column, Figure 7 and Figures S14 – S17 in the SI). Generally, the surface morphology was similar to that obtained at constant potentials, although the deposition method influences on the size, the number of nanostructures or their porosity. The surface nanostructures were essentially the same for **1Na-PheDOT** and **9Ant-PheDOT**, independently on the method of electropolymerization (cf. Figure 4 vs. 7 (middle and right columns) and Figures S6, S7 vs. S14, S15 in the SI). In contrast to that, whereas the vertically aligned nanotubes were formed in potentiodynamic polymerization of **2Na-PheDOT**, their number was smaller than in potentiostatic deposition and they did not cover the whole surface. Better control over nanotube formation in potentiostatic conditions (as compared to potentiodynamic conditions) was recently shown for electropolymerization of thienothiophene derivatives.[20] Electropolymerization of the dimer **(2Na-PheDOT)$_2$** in potentiodynamic conditions also led to the less uniform surface of the closed caps as compared to its potentiostatic electropolymerization (Figure 6, left vs. right column).

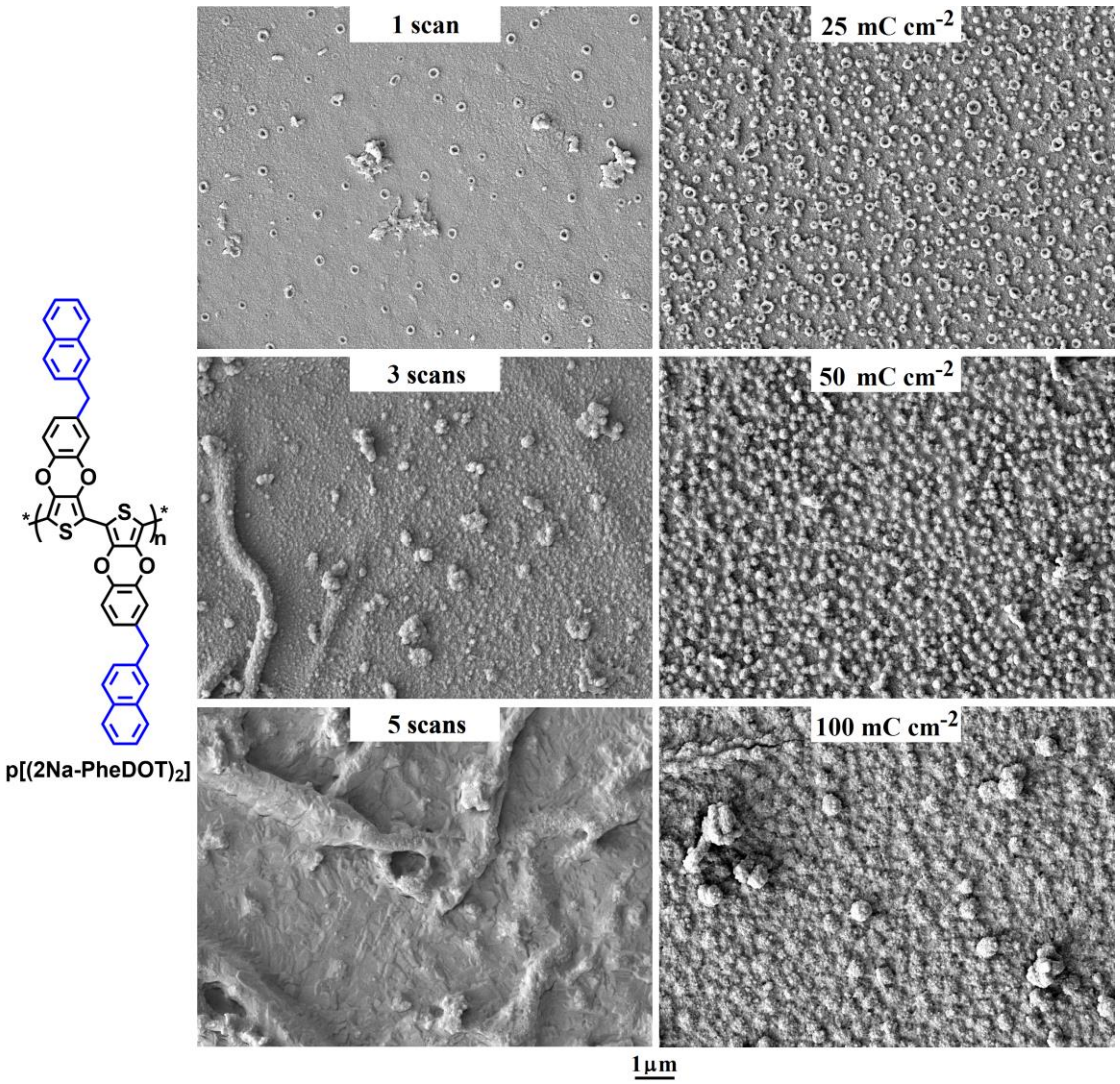


Figure 6. SEM images of the polymer surfaces electrodeposited from the dimer **(2Na-PheDOT)$_2$** (0.5 mM) in 0.1 M Bu_4NClO_4 / DCM in potentiodynamic conditions by cyclic voltammetry (E = –1 / +1.67 V) after 1, 3 and 5 scans (left), and in potentiostatic conditions at constant potential of E^{ox} = 1.67 V and the deposition charges of Q_s = 25, 50 and 100 mC cm^{-2} (right). Magnification: ×10,000.

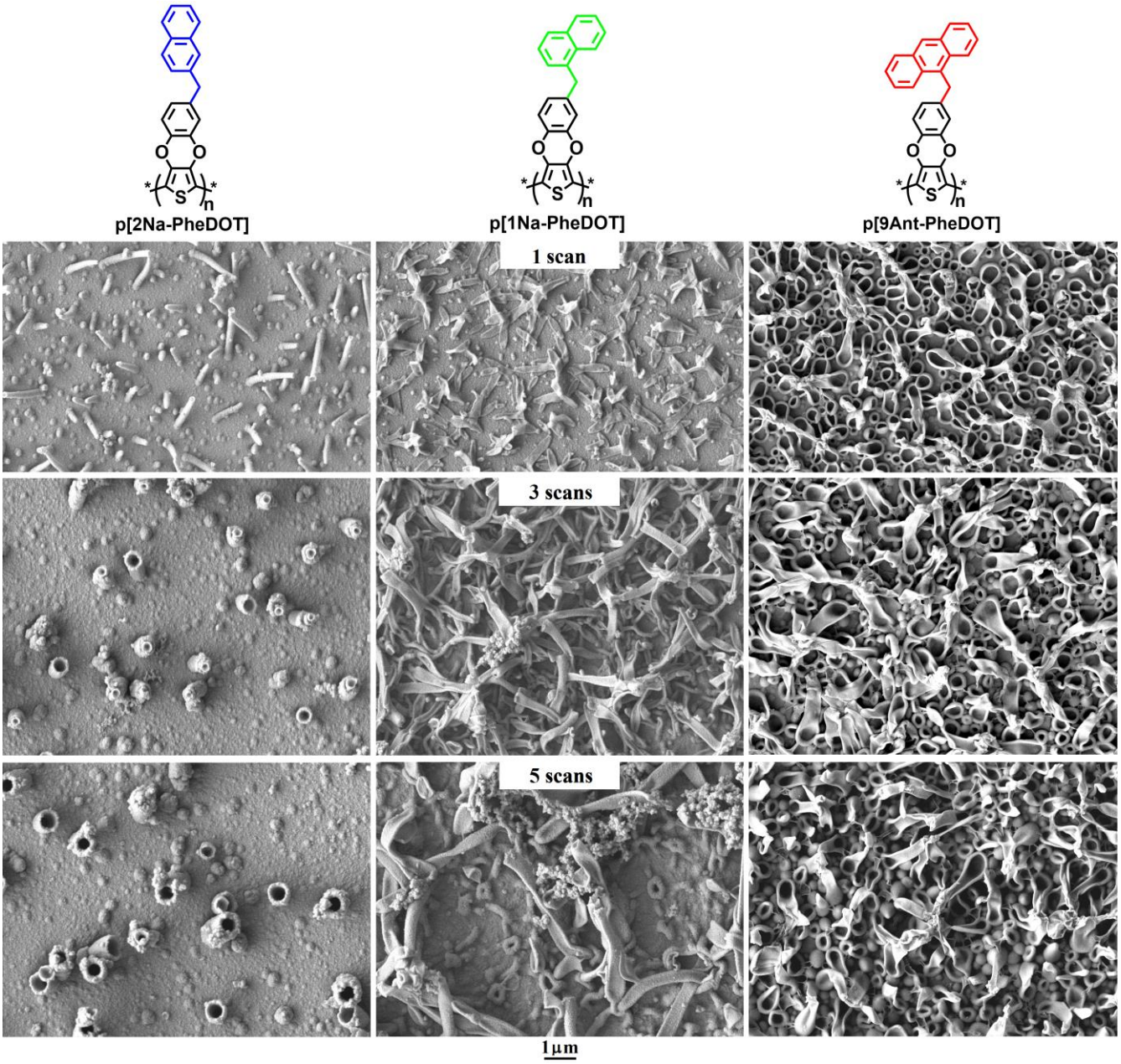


Figure 7. SEM images of the polymer surfaces electrodeposited from the monomers **2Na-PheDOT**, **1Na-PheDOT** and **9Ant-PheDOT** (10 mM) in 0.1 M Bu_4NClO_4 / DCM by cyclic voltammetry (E = –1 / + 1.70–1.80 V *vs.* SCE) after 1, 3 and 5 scans. Magnification: ×10,000.

Influence of the electrolyte. It is known that the medium used for electropolymerization can affect the morphology of the growing polymer films, and both the solvent[25,79] and the electrolyte[25,68] can affect the formed nanostructures. While both ClO_4^- and PF_6^- are weakly coordinating anions[80] (but PF_6^- is more hydrophobic), the difference on their effect on the surface structure of electropolymerized films in DCM was recently shown, e.g. for **NaphDOT**[68] (Figure 1) or **2Na-PheDOT**.[70] For

electropolymerization with Bu_4NPF_6 salt as an electrolyte, formation of ordered nanotubes was less favored giving much rougher and inhomogeneous disordered surfaces. This difference is intuitively expected to be more pronounced in less polar solvent. Really, much weaker effect of the electrolyte (with weakly-coordinating anions ClO_4^- and BF_4^-) was observed for polymerization of **EDOT** in polar solvent (acetonitrile or propylene carbonate).[79]

Electrodeposition of **1Na-PheDOT** in Bu_4NClO_4 / DCM showed initial formation of ordered nanostructures on the surface at low deposition charge, but when Q_c increased, they quickly collapsed and aggregated to form structureless sponge-like surface (Figures S18 and S19 in the SI). It was surprisingly, therefore, to observe different behavior of the dimer **(2Na-PheDOT)$_2$** when the electrolyte changed from Bu_4NClO_4 to Bu_4NPF_6 (Figure 8 and Figures S20 and S21 in the SI). Fast agglomeration and growing 3D spherical nanoparticles was observed with Bu_4NClO_4 (Figure 6) and we expected even smoother surface in the case of Bu_4NPF_6. However, while the surface was tight, with increasing the deposition charge at constant potential, the large spherical holes were formed on the surface (~ 400 – 1000 nm) creating the membrane structure of **p[(2Na-PheDOT)$_2$]** polymer film (Figure 8 and Figures S20 in the SI). Similar nanoholes were also observed after 1 scan of potentiodynamic deposition by CV, but they collapsed and filled in quickly with the growing polymer on next scans to produce smooth surface (Figure S21 in the SI).

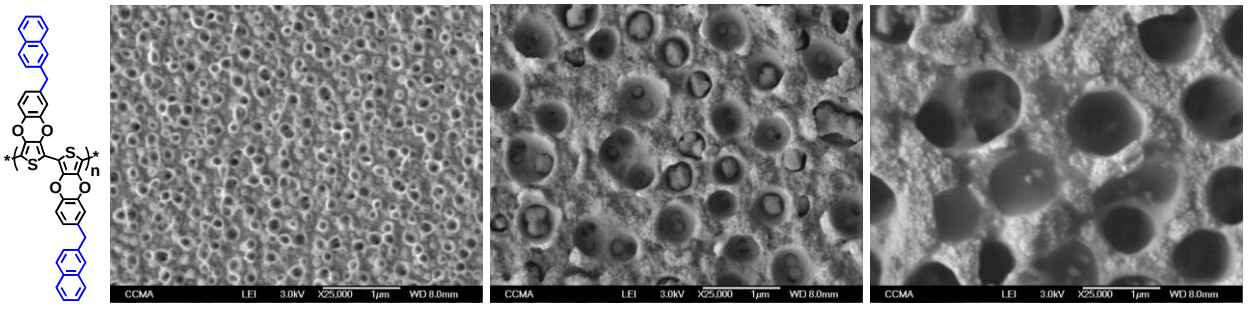


Figure 8. SEM images of the polymer surfaces electrodeposited from the dimer **(2Na-PheDOT)$_2$** (0.5 mM) in 0.1 M Bu_4NPF_6 / DCM in potentiostatic conditions at constant potential of E^{ox} = 1.67 V and the deposition charges of Q_s = 25, 100 and 400 mC cm^{-2} (from the left to the right). Magnification: ×25,000.

Water effect on the surface morphology. Previously we mentioned that traces of water in the solvent, which generate O_2 and H_2 gas bubbles on the surface during the electropolymerization is an important factor for the formation of the polymer nanostructures. This is in line with previous report in the literature. Thus, Shi and co-workers demonstrated formation of large vertically aligned hollow tubules

(~50 – 200 μm in diameter) with opened tops in polymerization of pyrrole in aqueous media.[14,15,22] They explained the observed results as formation of gas bubbles on the surface of polypyrrole film and growing the polymer films around these bubbles. Similar results were observed by other authors with the same explanation of the mechanism of their formation.[81,82,83] In polymerization of pyrrole in aqueous solution in the presence of surfactant, growing of the polymer around of gas bubbles can also result in formation of hollow spherical or bowl-like microcontainers (d ~ 2 – 70 μm).[84,85]

Very recently, we have studied the influence of water on the surface morphology of electrodeposited polymers from thieno[3,4-*b*]thiophene derivatives.[86,87] It has been demonstrated that with significant amount of water in dichloromethane (dichloromethane saturated with water *vs.* commercial dichloromethane) the surface morphology is drastically changed, e.g. from densely packed spherical particles to nanoporous membrane structures (with pores of d ~ 100 – 300 nm)[86] or from smooth or tree-like surfaces to hollow spherical or coral-like structures.[87] This is likely to be due to the formation of a large amount a gas bubbles (O_2 and H_2) during electropolymerization in dichloromethane/water system.

We have investigated the effect of water on the surface morphology of the polymer films obtained from **2Na-PheDOT**. In dichloromethane solution (with only traces of water in it), this monomer formed long vertically aligned nanotubes (Figures 4, 5, and 7). When dichloromethane saturated with H_2O was used as a solvent, the surface nanostructure changed drastically (Figures 9 and Figures S22 and S23 in the SI). Due to significant amount of water, the gas bubbles started to form more intensely, leading to large amount of tightly spaced hemisphere nanostructures on the surface (d ~ 100 – 300 nm) to form membrane-type structure of the polymer film. With an increase of the number of scans in potentiodynamic polymerization, the size of these nanocups increased to 600 – 1000 nm, while their number decreased due to flattening the surface between them. Although they were not aligned perfectly, their shape clear indicated that the mechanism of their formation can be described as growing polymer shells around the gas bubbles adhered on the surface. They did not form closed spherical containers, as was observed e.g. for pyrrole electropolymerization in aqueous solution with surfactants,[84,85] but remained as opened hemispheres. This supports the mechanism of nanostructures formation with studied **PheDOT** derivatives and emphasize the importance of has bubbles formation during the electropolymerization process.

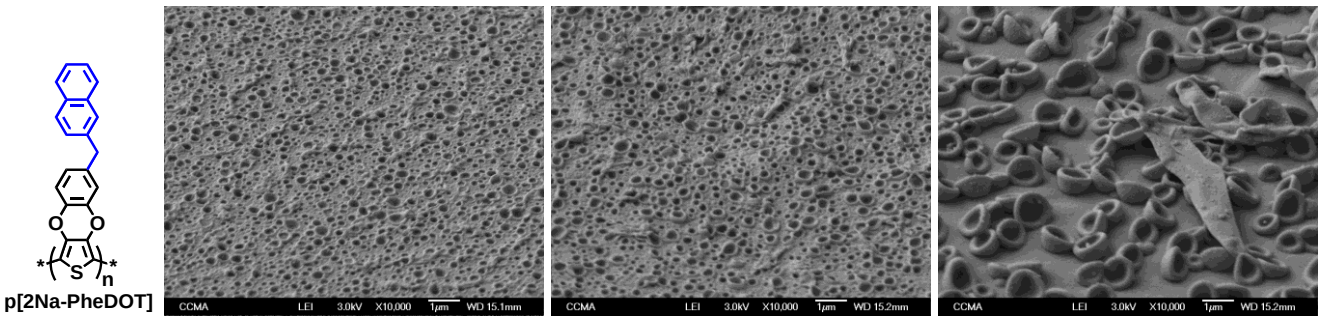


Figure 9. SEM images of the **p[2Na-PheDOT]** polymer surfaces obtained by electropolymerization of **2Na-PheDOT** (10 mM) in 0.1 M Bu_4NClO_4 / (DCM + H_2O) in potentiodynamic conditions by cyclic voltammetry (E = –1 / +1.8 V) after 1, 3 and 5 scans of depositions (from the left to the right). Substrate inclination: 45 °; magnification: ×10,000.

Surface wettability

The apparent contact angles (θ_w) and the surface roughness (Ra and Rq) of the electrodeposited polymer films are summarized in Tables 1 and 2. First of all, the surfaces obtained with **9Ant-PheDOT** are all hydrophilic with some decrease of θ_w as a function of the deposition charge. The results are easy to explain using the Wenzel equation, which describes the case where the water droplet enters in all the surface roughness (full wetting) leading to a full solid–liquid interface. The Wenzel equation (5)[88] is given as:

$$\cos\theta = r\cdot\cos\theta^{Y}, \qquad (5)$$

where r is the roughness parameter and θ^Y is the contact angle of the smooth surface. Here, the polymers are intrinsically hydrophilic ($\theta^Y{}_w$) and as a consequence it is expected that θ_w decreases when r increases.

However, some surfaces obtained in potentiostatic conditions are highly hydrophobic, for example the surfaces obtained from **2Na-PheDOT** at low deposition charge **(large number of nanotubes)** or from **1Na-PheDOT** at high deposition charge **(large number of nanoribbons)**. These results can only be explained using the Cassie-Baxter model, indicating the presence of the air trapped inside the surface roughness. Indeed, the Cassie–Baxter equation (6)[89] is written as:

$$\cos\theta = r_f\cdot f\cdot\cos\theta^{Y} + f - 1, \qquad (6)$$

where r_f is the roughness factor of the solid fraction in contact with the wetting liquid (the ratio of actual surface area to the planar surface) and f is the fraction of the surface wetted by the liquid [thus, $(1 - f)$ is the air fraction].

Table 1. Surface roughness and apparent contact angles of different polymers as a function of the number of deposition charge at constant potential.[a]

Monomer (concentration)[b]	Deposition charge [mC cm^{-2}]	Ra [nm][c]	Rq [nm][c]	θ_w [deg][d]
2Na-PheDOT (10 mM)	12.5	10 ± 3	19 ± 6	119 ± 2
	25	9 ± 2	13 ± 2	97 ± 7
	50	19 ± 10	33 ± 21	113 ± 3
	100	388 ± 26	488 ± 31	52 ± 15
	200	494 ± 34	631 ± 45	28 ± 6
	400	613 ± 94	825 ± 110	0
(2Na-PheDOT)$_2$ (0.5 m M)	12.5	10 ± 2	15 ± 4	86 ± 2
	25	12 ± 1	32 ± 6	87 ± 2
	50	29 ± 6	68 ±12	82±1
	100	44 ± 10	90 ±20	101±1
	200	210 ± 30	310 ±50	75 ± 2
	400	400 ± 35	540 ±50	90 ± 5
1Na-PheDOT (10 mM)	12.5	16 ± 2	23 ± 4	61 ± 1
	25	38 ± 4	54 ± 5	50 ± 5
	50	56 ± 4	81 ± 7	60 ± 6
	100	300 ± 15	400 ± 7	53 ± 4
	200	560 ± 24	720 ± 30	44 ± 4
	400	255 ± 8	328 ± 15	127 ± 3
9Ant-PheDOT (10 mM)	12.5	123 ± 25	230 ±32	60 ± 1
	25	147 ± 26	216 ± 30	63 ± 1
	50	347 ± 60	481 ± 72	55 ± 2
	100	456 ± 22	600 ± 20	47 ± 3
	200	344 ± 28	472 ± 33	47 ± 2
	400	434 ± 34	557 ± 38	41 ± 2

[a]Electrodeposition was performed in 0.1 M Bu_4NClO_4 / DCM. [b]Monomers used for electropolymerization and their concentrations. [c]Ra and Rq are arithmetic and quadratic roughness of the polymer surface, respectively. [d]θ_w is an apparent contact angle of the water droplet with the polymer surface.

In this case, according to the above equation, the contact angle θ can be increased even if the polymer forming the surface is intrinsically hydrophilic. For example, completely "smooth" surfaces obtained with **2Na-PheDOT** are highly hydrophilic with $\theta^Y_w = 57.5°$.[70] For small deposition charge of Qs = 12.5 mC cm^{-2}, although the surface roughness was low, a very high θ_w of up to 119° was observed because of the presence of densely-packed nanotubular seeds of the size less than 100 nm. The change from hydrophilic to hydrophobic surface with the same material is possible because of the presence of densely-packed nanotubular seeds which allow trapping high amount of air between the surface and the

water droplet (Cassie-Baxter equation (6)).[89] When Qs increased, an increase in the tubes height and diameter was observed, but the number of open nanotubes was decreased (Figure 4, left column). As a consequence, θ_w discontinuously decreased until the surface became superhydrophilic (Table 1) (Wenzel equation (5)).[88] With **1Na-PheDOT**, the wetting properties were clearly different because the structures are not porous (2D/3D ribbon-like structures). Here, an increase in the ribbon length and edge with an increase of Qs was observed. At high deposition charge of Qs = 400 mC cm^{-2}, large amount of air can be trapped between the long ribbon-like structures (Cassie-Baxter equation (6)),[89] so the surfaces became hydrophobic (θ_w = 127°).

Table 2. Surface roughness and apparent contact angles of different polymers as a function of the number of deposition scans by cyclic voltammetry.[a]

Monomer (concentration)[b]	Number of deposition scans	Ra [nm]	Rq [nm]	θ_w [deg]
2Na-PheDOT (10 mM)	1	47 ± 8	62 ± 11	104 ± 4
	3	53 ± 16	96 ± 40	110 ± 4
	5	57 ± 8	84 ± 12	103 ± 2
(2Na-PheDOT)$_2$ (0.5 mM)	1	28 ± 6	39 ± 12	110 ± 1
	3	156 ± 10	226 ± 23	56 ± 4
	5	192 ± 9	280 ± 13	77 ± 10
1Na-PheDOT (10 mM)	1	45 ± 3	59 ± 4	88 ± 3
	3	159 ± 5	238 ± 30	134 ± 2
	5	225 ± 10	320 ± 7	133 ± 1
9Ant-PheDOT (10 mM)	1	86 ± 20	104 ± 22	76 ± 2
	3	200 ± 10	257 ± 15	120 ± 3
	5	380 ± 70	504 ± 90	129 ± 1

[a]Electrodeposition was performed in 0.1 M Bu_4NClO_4 / DCM. [b]Monomers used for electropolymerization and their concentrations.

The polymer surface obtained from **2Na-PheDOT** by cyclic voltammetry is slightly hydrophobic whatever the number of scans (Table 2). This is due to the fact that the number of tubes is not extremely important in this case whereas the distance between them is a crucial factor. By contrast, the presence of ribbon-like nanostructures for the polymer from **1Na-PheDOT** induces more pronounced increase in the surface hydrophobicity with θ_w up to 134 °. Moreover, the surface is completely sticky (parahydrophobic): water droplets placed on this surface did not move whatever the surface inclination (Figure 10) indicating of very strong water adhesion, as observed, for example, on rose petals. Hence, the presence of ribbon-like structures might have a huge influence on the surface hydrophobicity because the air trapped below them can be very important, depending on the dimensions and the

position of the nanostructures. Similar changes in the surface hydrophobicity with an increase of contact angle from θ_w = 76 ° (1 scan) to θ_w = 129 ° (5 scans) was observed for **9Ant-PheDOT**, where ribbon-like structures started to form progressively with the scans (Figure 7, right column and Figures S14 – S17 in the SI). In the case **(2Na-PheDOT)$_2$**, slightly hydrophobic surface was obtained after 1 scan, but the surface became hydrophilic when the number of scans increases.



Figure 10. The photograph of water droplet on the surface of **p[1Na-PheDOT]** polymer electrochemically prepared in 0.1 M Bu_4NClO_4 / DCM by cyclic voltammetry (E = –1 / +1.70 V; 5 scans) and inclined at the angle of 90 °.

Conclusions

We have designed and successfully synthesized a series of functionalized 3,4-phenylenedioxythiophene monomers with different substituents at the benzene ring (2- and 1-naphtylmethyl-, and 9-anthracenylmethyl-: **2Na-PheDOT**, **1Na-PheDOT** and **9Ant-PheDOT**), as well as the dimer **(2Na-PheDOT)$_2$** and the trimer **(2Na-PheDOT)$_3$**. Their electropolymerization (in either potentiostatic or potentiodynamic conditions, in 0.1 M Bu_4NClO_4 / DCM) results in polymer surfaces of different morphologies. We have demonstrated that even small variations in the structure of the side polynuclear aromatic moieties in these monomers lead to drastic changes in the formed polymer surface nanostructures. Thus, the polymer growth from **2Na-PheDOT** is monodirectional (1D) to form vertically aligned nanotubes (d ~ 300 –500 nm), **1Na-PheDOT** gives ribbon-like nanostructures of up to 10 – 15 μm in length with 300 – 800 nm in width (2D growth), and **9Ant-PheDOT** forms a mixture of these two structures. These differences in the formed nanostructures lead to different hydrophobicity of the surface, from hydrophilic to parahydrophobic, achieving the water droplet contact angles θ_w of up to 129 – 134 ° and very strong water adhesion (for **1Na-PheDOT** and **9Ant-PheDOT**). Moreover, we showed that in the case of **2Na-PheDOT** monomer and **(2Na-PheDOT)$_2$** dimer, which formally give the polymer of the same chemical structure, the growth of the nanostructures is very different.

Instead of vertically aligned nanotubes (as in the case of **2Na-PheDOT**), the dimer **(2Na-PheDOT)$_2$** forms the surface with only spherical particles (3D) that can be attributed to its very low solubility and faster electropolymerization rate. Moreover, changing the electrolyte to Bu_4NPF_6, drastically change the surface from the dimer **(1Na-PheDOT)$_2$** to create the membrane structure with 400 – 1000 nm spherical holes. We also demonstrated an influence of the conditions of electropolymerization (potentiostatic or potentiodynamic) and content of water in dichloromethane on the surface morphology and wettability, arising from different conditions for gas bubbles formation (O_2 or H_2) during the polymer growth.

Experimental Part

All commercial chemicals and solvents were used as received from Aldrich, Alfa Aesar, or Fisher, without further purification. Details of synthetic procedures and characterizations of all novel compounds shown in the Schemes 1 – 3 are given in the SI.

Cyclic voltammetry and electrodeposition experiments

The electrochemical depositions were performed with a Metrohm Autolab Potentiostat Model PGSTAT100. The electrochemical experiments were performed by three-electrode scheme consisting of a gold plate (2 cm^2) as the working electrode, a carbon-rod as the counter electrode and a saturated calomel electrode (SCE) as the reference electrode. The three electrodes were placed into the electrochemical cell, 10 mL of dichloromethane with 0.1 M of tetrabutylammonium perchlorate (Bu_4NClO_4) or hexafluorophosphate (Bu_4NPF_6) as an electrolyte was added to the cell and the cell was degassed with argon. Then, the monomer with a precise concentration was added to this solution. The monomer oxidation potential (E^{ox}) was determined by cyclic voltammetry. Afterwards, the depositions were performed either in potentiodynamic conditions by cyclic voltammetry (scan rate: 20 mV s^{-1}; number of scans: 1, 3 and 5) or in potentiostatic conditions at constant potential ($E = E^{ox}$; deposition charge Q_s = 12.5, 25, 50, 100, 200 and 400 mC cm^{-2}). Afterthat, the substrates with the deposited polymer films were washed three times with dichloromethane and slowly dried, before studies their surfaces by SEM. For studies of water influence on the surface morphology, an excess of water was added to commercial dichloromethane, stirred and left to stay for phase separation. Water layer was separated from dichloromethane by decantation and dichloromethane saturated with H_2O was used in experiments, similarly to that described above. For electrochemical characterization of electrodeposited polymers, the monomers were electropolymerized on the gold plate (2 cm^2) working electrode as

described above. The electrodeposited polymer films were washed with dichloromethane and their electrochemical response was then studied in a monomer-free 0.1 M Bu_4NClO_4 / dichloromethane solution using the same three-electrode scheme.

Surface characterization

The surface morphology was investigated by scanning electron microscopy using a JEOL 6700F microscope. The surface roughness (arithmetic Ra and quadratic Rq) was determined by optical profilometry using a Wyko NT 1100 optical microscope (Bruker) and the "Vision" software. The measurements were performed in the High Mag Phase Shift Interference (PSI) working mode, field of view 0.5× and objective 50×. For the surface wetting properties, a DSA30 goniometer (Kruss) and the "Drop Shape Analysis System" software were used. The apparent contact angles (θ_w) were obtained with the sessile droplet method with 2 µL water droplets. The dynamic contact angles were obtained by the tilted droplet method using 6 µL water droplets. The surface was inclined and the maximum angle achieved before the droplet moves was measured. This angle is also called as sliding angle (α). If the droplet does not move after an inclination of 90º, the water adhesion is extremely strong and the surface is called sticky.

ASSOCIATED CONTENT

Supporting Information

The Supporting Information is available free of charge on the

ACS Publications website at DOI: 10.1021/acsmacromol.XXXXXX

Experimental procedures for synthesis of new compounds, copies of ^1H and ^{13}C NMR, and MS spectra of new compounds, cyclic voltammograms of polymers, DFT optimized structures for monomers, SEM images of polymer surfaces (PDF).

AUTHOR INFORMATION

Corresponding Authors:

*E-mail: thierry.darmanin@unice.fr (T.D.)

*E-mail: i.perepichka@nwpu.edu.cn (I.F.P.); i.perepichka@bangor.ac.uk (I.F.P)

ORCHID

Thierry Darmanin: 0000-0003-0150-7412

Elena L. Klimareva: 0000-0002-2306-1354

Frédéric Guittard: 0000-0001-9046-6725

Igor F. Perepichka: 0000-0001-6672-3103

Notes

There authors declare no competing financial interests.

ACKNOWLEDGEMENTS

The authors thank the Centre Commun de Microscopie Appliquée (CCMA, Univ. Nice Sophia Antipolis) for the realization of the SEM images. E.L.K. thanks the Russia President PhD Scholarship for studying abroad to visit Bangor University and to Act 211 Government of the Russian Federation for financial support (contract No 02.A03.21.0006). I.S. thanks the Erasmus+ student mobility program for supporting her internship at Bangor University. I.F.P. thanks to SIFE-NPU for generous startup funding.

References

(1) Yu, S.; Guo, Z.; Liu, W. Biomimetic Transparent and Superhydrophobic Coatings: From Nature and Beyond Nature. *Chem. Commun.* **2015**, *51*, 1775–1794.

(2) Darmanin, T.; Guittard, F. Recent Advances in the Potential Applications of Bioinspired Superhydrophobic Materials. *J. Mater. Chem. A* **2014**, *2*, 16319–16359.

(3) Dong, Z.; Schumann, M. F.; Hokkanen, M. J.; Chang, B.; Welle, A.; Zhou, Q.; Ras, R. H. A.; Xu, Z.; Wegener, M.; Levkin, P. A. Superoleophobic Slippery Lubricant-Infused Surfaces: Combining Two Extremes in the Same Surface. *Adv. Mater.* **2018**, *30*, 18803890.

(4) Heng, X.; Xiang, M.; Lu, Z.; Luo, C. Branched ZnO Wire Structures for Water Collection Inspired by Cacti. *ACS Appl. Mater. Interfaces* **2014**, *6*, 8032−8041.

(5) Ju, J.; Bai, H.; Zheng, Y.; Zhao, T.; Fang, R.; Jiang, L. A Multi-Structural and Multi-Functional Integrated Fog Collection System in Cactus. *Nat. Commun.* **2012**, *3*, 1247.

(6) Popova, A. A.; Schillo, S. M.; Demir, K.; Ueda, E.; Nesterov-Mueller, A.; Levkin, P. A. Droplet-Array (DA) Sandwich Chip: A Versatile Platform for High-Throughput Cell Screening Based on Superhydrophobic–Superhydrophilic Micropatterning. *Adv. Mater.* 2015, *27*, 5217–5222.

(7) Wasay, A.; Sameoto, D. Gecko Gaskets for Self-Sealing and High-Strength Reversible Bonding of Microfluidics, *Lab. Chip* **2015**, *15*, 2749−2753.

(8) Ganesh, V. A.; Raut, H. K.; Nair, A. S.; Ramakrishna, S. A Review on Self-Cleaning Coatings. *J. Mater. Chem.* **2011**, *21*, 16304–16322.

(9) Liu, K.; Jiang, L. Bio-Inspired Self-Cleaning Surfaces. *Annu. Rev. Mater. Res.* 2012, *42*, 231–263.

(10) Geyer, F. L.; Ueda, E.; Liebel, U.; Grau, N.; Levkin, P. A. Superhydrophobic–Superhydrophilic Micropatterning: Towards Genome-on-a-Chip Cell Microarrays. *Angew. Chem. Int. Ed.* **2011**, *50*, 8424–8427.

(11) Darmanin, T.; Guittard, F. Wettability of Conducting Polymers: From Superhydrophilicity to Superoleophobicity. *Progr. Polym. Sci.* **2014**, *39*, 656–682.

(12) Mortier, C.; Darmanin, T.; Guittard, F. 3,4-Ethylenedioxypyrrole (EDOP) Monomers with Aromatic Substituents for Parahydrophobic Surfaces by Electropolymerization. *Macromolecules* **2015**, *48*, 5188−5195.

(13) Parakhonskiy, B.; Shchukin, D. Polypyrrole Microcontainers: Electrochemical Synthesis and Characterization. *Langmuir* **2015**, *31*, 9214−9218.

(14) Yuan, J.; Qu, L.; Zhang, D.; Shi, G. Linear Arrangements of Polypyrrole Microcontainers. *Chem. Commun.* **2004**, 994−995.

(15) Qu, L.; Shi, G.; Chen, F.; Zhang, J. Electrochemical Growth of Polypyrrole Microcontainers. *Macromolecules* **2003**, *36*, 1063−1067.

(16) Debiemme-Chouvy, C. One-Step Electrochemical Synthesis of a Very Thin Overoxidized Polypyrrole. *Electrochem. Solid-State Lett.* **2007**, *10*, E24−E26.

(17) Fakhry, A.; Cachet, H.; Debiemme-Chouvy, C. Mechanism of Formation of Templateless Electrogenerated Polypyrrole Nanostructures, *Electrochim. Acta* **2015**, *179*, 297−303.

(18) Fakhry, A.; Pillier, F.; Debiemme-Chouvy, C. Templateless Electrogeneration of Polypyrrole Nanostructures: Impact of the Anionic Composition and pH of the Monomer Solution. *J. Mater. Chem. A* **2014**, *2*, 9859−9865.

(19) Bai, S.; Hu, Q.; Zeng, Q.; Wang, M.; Wang, L. Variations in Surface Morphologies, Properties, and Electrochemical Responses to Nitro-Analyte by Controlled Electropolymerization of Thiophene Derivatives. *ACS Appl. Mater. Interfaces* **2018**, *10*, 11319−11327.

(20) Chagas, G. R.; Darmanin, T.; Guittard, F. One-Step and Templateless Electropolymerization Process Using Thienothiophene Derivatives To Develop Arrays of Nanotubes and Tree-like Structures with High Water Adhesion. *ACS Appl. Mater. Interfaces* **2016**, *8*, 22732−22743.

(21) Mortier, C.; Darmanin, T.; Guittard, F. 3,4-Dialkoxypyrrole for the Formation of Bioinspired Rose Petal-like Substrates with High Water Adhesion. *Langmuir* **2016**, *32*, 12476−12487.

(22) Qu, L.; Shi, G.; Yuan, J.; Han, G.; Chen, F. Preparation of Polypyrrole Microstructures by Direct Electrochemical Oxidation of Pyrrole in an Aqueous Solution of Camphorsulfonic Acid. *J. Electroanal. Chem.* **2004**, *561*, 149–156.

(23) Wolfs, M.; Darmanin, T.; Guittard, F. Superhydrophobic Nanofiber Arrays and Flower-like Structures of Electrodeposited Conducting Polymers. *Soft Matter* **2012**, *8*, 9110–9114.

(24) Luo, S.-C.; Liour, S. S.; Yu, H.-h. Perfluoro-Functionalized PEDOT Films with Controlled Morphology as Superhydrophobic Coatings and Biointerfaces with Enhanced Cell Adhesion. *Chem. Commun.* **2010**, *46*, 4731–4733.

(25) Wolfs, M.; Darmanin, T.; Guittard, F. Versatile Superhydrophobic Surfaces from a Bioinspired Approach. *Macromolecules* **2011**, *44*, 9286–9294.

(26) Mortier, C.; Darmanin, T.; Guittard, F. Parahydrophobic Surfaces Made of Intrinsically Hydrophilic PProDOT Nanofibers with Branched Alkyl Chains. *Adv. Eng. Mater.* 2014, **16**, 1400–1405.

(27) Chang, J. H.; Hunter, I. W. A Superhydrophobic to Superhydrophilic In Situ Wettability Switch of Microstructured Polypyrrole Surfaces. *Macromol. Rapid Commun.* **2011**, *32*, 718–723.

(28) Wolfs, M.; Darmanin, T.; Guittard, F. Superhydrophobic Fibrous Polymers. *Polym. Rev.* **2013**, *53*, 460–505.

(29) Darmanin, T.; Guittard, F. Molecular Design of Conductive Polymers To Modulate Superoleophobic Properties. *J. Am. Chem. Soc.* **2009**, *131*, 7928–7933.

(30) Darmanin, T.; Guittard, F. Highly Hydrophobic Films With Various Adhesion by Electrodeposition of Poly(3,4-bis(alkoxy)thiophene)s. *Soft Matter* **2013**, *9*, 1500–1505.

(31) El Kout, E.; Trad, R. B.; El Kateb, M.; Beji, M.; Laugier, J.-P.; Godeau, G.; Guittard, F.; Darmanin, T. Combining Staudinger Reductive Amination and Amidification for the Control of Surface Hydrophobicity and Water Adhesion by Introducing Heterobifunctional Groups: Post- and Ante-Approach. *Macromol. Chem. Phys.* **2017**, *218*, 1700250.

(32) Perepichka, I. F.; Perepichka, D. F. (eds.), *Handbook of Thiophene-Based Materials: Applications in Organic Electronics and Photonics*, 2-Volume Set, John Wiley & Sons: Chichester, **2009**, 910 pages, ISBN: 978-0470057322s.

(33) Perepichka, I. F.; Perepichka, D. F.; Meng, H.; Wudl, F. Light Emitting Polythiophenes. *Adv. Mater.* **2005**, *17*, 2281–2305.

(34) Groenendaal, L. "Bert"; Jonas, F.; Freitag, D.; Pielartzik, H.; Reynolds, J. R. Poly(3,4-ethylenedioxythiophene) and Its Derivatives: Past, Present, and Future. *Adv. Mater.* **2000**, *12*, 481–494.

(35) Kirchmeyer, S.; Reuter, K. Scientific Importance, Properties and Growing Applications of Poly(3,4-ethylenedioxythiophene). *J. Mater. Chem.* **2005**, *15*, 2077–2088.

(36) Reuter, K.; Kirchmeyer, S.; Elschner, A. PEDOT – Properties and Technical Relevance. In Book: *Handbook of Thiophene-Based Materials: Applications in Organic Electronics and Photonics*, Perepichka, I. F.; Perepichka, D. F. (eds.), John Wiley & Sons: Chichester, **2009**, Chapter 14, p. 549–576.

(37) Elschner, A.; Kirchmeyer, S.; Lovenich, W.; Merker, U.; Reuter, K. *PEDOT: Principles and Applications of an Intrinsically Conductive Polymer*, CRC Press: Boca Raton, **2010**, 377 pages, ISBN 978-1420069112.

(38) Raimundo, J.-M.; Blanchard, P.; Frère, P.; Mercier, N.; Ledoux-Rak, I.; Hierle, R.; Roncali, J. Push–pull Chromophores Based on 2,2'-Bi(3,4-ethylenedioxythiophene) (BEDOT) π-Conjugating Spacer. *Tetrahedron Lett.* **2001**, *42*, 1507–1510.

(39) Leriche, P.; Turbiez, M.; Monroche, V.; Frère, P.; Blanchard, P.; Skabara, P. J.; Roncali, J. Strong π-Electron Donors Based on a Self-Rigidified 2,2'-Bi(3,4-ethylenedioxy)thiophene–Tetrathiafulvalene Hybrid π-Conjugated System. *Tetrahedron Lett.* **2003**, *44*, 649–652.

(40) Turbiez, M.; Frère, P.; Roncali, J. Stable and Soluble Oligo(3,4-ethylenedioxythiophene)s End-Capped with Alkyl Chains. *J. Org. Chem.* **2003**, *68*, 5357–5360.

(41) Turbiez, M.; Frère, P.; Allain, M.; Videlot, C.; Ackermann, J.; Roncali, J. Design of Organic Semiconductors: Tuning the Electronic Properties of π-Conjugated Oligothiophenes with the 3,4-Ethylenedioxythiophene (EDOT) Building Block. *Chem. Eur. J.* **2005**, *11*, 3742–3752.

(42) McEntee, G. J.; Skabara, P. J.; Vilela, F.; Tierney, S.; Samuel, I. D. W.; Gambino, S.; Coles, S. J.; Hursthouse, M. B.; Harrington, R. W.; Clegg, W. Synthesis and Electropolymerization of Hexadecyl Functionalized Bithiophene and Thieno[3,2-*b*]thiophene End-Capped with EDOT and EDTT Units. *Chem. Mater.* **2010**, *22*, 3000–3008.

(43) Nalin de Silva, K. M.; Hwang, E.; Serem, W. K.; Fronczek, F. R.; Garno, J. C.; Nesterov, E. E. Long-Chain 3,4-Ethylenedioxythiophene/Thiophene Oligomers and Semiconducting Thin Films Prepared by Their Electropolymerization. *ACS Appl. Mater. Interfaces* **2012**, *4*, 5430–5441.

(44) Wijsboom, Y. H.; Patra, A.; Zade, S. S.; Sheynin, Y.; Li, M.; Shimon, L. J. W.; Bendikov, M. Controlling Rigidity and Planarity in Conjugated Polymers: Poly(3,4-ethylenedithioselenophene). *Angew. Chem. Int. Ed.* **2009**, *48*, 5443 –5447.

(45) Leriche, P.; Blanchard, P.; Frère, P.; Levillain, E.; Mabon, G.; Roncali, J. 3,4-Vinylenedioxythiophene (VDOT): a New Building Block for Thiophene-Based π-Conjugated Systems. *Chem. Commun.* **2006**, 275–277.

(46) Spencer, H. J.; Skabara, P. J.; Giles, M.; McCulloch, I.; Coles, S. J.; Hursthouse, M. B. The First Direct Experimental Comparison Between the Hugely Contrasting Properties of PEDOT and the All-Sulfur Analogue PEDTT by Analogy with Well-Defined EDTT–EDOT Copolymers. *J. Mater. Chem.* **2005**, *15*, 4783–4792.

(47) Turbiez, M.; Hergué, N.; Leriche, P.; Frère, P. Rigid Oligomers Based on the Combination of 3,6-dimethoxy-thieno[3,2-*b*]thiophene and 3,4-Ethylenedioxythiophene. *Tetrahedron Lett.* **2009**, *50*, 7148–7151.

(48) Dong, T.; Lv, L.; Feng, L.; Xia, Y.; Deng, W.; Ye, P.; Yang, B.; Ding, S.; Facchetti, A.; Dong, H.; Huang, H. Noncovalent Se···O Conformational Locks for Constructing High-Performing Optoelectronic Conjugated Polymers. *Adv. Mater.* **2017**, *29*, 1606025.

(49) Thorley, K. J.; McCulloch, I. Why Are S–F and S–O Non-Covalent Interactions Stabilising?, *J. Mater. Chem. C* **2018**, *6*, 12413–12421.

(50) Conboy, G.; Spencer, H. J.; Angioni, E.; Kanibolotsky, A. L.; Findlay, N. J.; Coles, S. J.; Wilson, C.; Pitak, M. B.; Risko, C.; Coropceanu, V.; Brédas, J.-L.; Skabara, P. J. To Bend or Not To Bend – Are Heteroatom Interactions within Conjugated Molecules Effective in Dictating Conformation and Planarity?. *Mater. Horiz.*, **2016**, *3*, 333–339.

(51) Medina, B. M.; Wasserberg, D.; Meskers, S. C. J.; Mena-Osteritz, E.; Bäuerle, P.; Gierschner, J. EDOT-Type Materials: Planar but Not Rigid. *J. Phys. Chem. A* **2008**, *112*, 13282–13286.

(52) Roncali, J.; Blanchard, P.; Frère, P. 3,4-Ethylenedioxythiophene (EDOT) as a Versatile Building Block for Advanced Functional π-Conjugated Systems. *J. Mater. Chem.* **2005**, *15*, 1589–1610.

(53) Luo, S.-C.; Ali, E. M.; Tansil, N. C.; Yu, H.-h.; Gao, S.; Kantchev, E. A. B.; Ying, J. Y. Poly(3,4-ethylenedioxythiophene) (PEDOT) Nanobiointerfaces: Thin, Ultrasmooth, and Functionalized PEDOT Films with in Vitro and in Vivo Biocompatibility. *Langmuir* **2008**, *24*, 8071–8077.

(54) Galán, T.; Prieto-Simón, B.; Alvira, M.; Eritja, R.; Götz, G.; Bäuerle, P.; Samitier, J. Label-Free Electrochemical DNA Sensor Using "Click"-Functionalized PEDOT Electrodes. *Biosensors Bioelectronics* **2015**, *74*, 751–756.

(55) Darmanin, T.; Guittard, F. Superoleophobic Surfaces with Short Fluorinated Chains? *Soft Matter* **2013**, *9*, 5982–5990.

(56) Darmanin, T.; Taffin de Givenchy, E.; Amigoni, S.; Guittard, F. Hydrocarbon versus Fluorocarbon in the Electrodeposition of Superhydrophobic Polymer Films. *Langmuir* **2010**, *26*, 17596–17602.

(57) Darmanin, T.; Nicolas, M.; Guittard, F. Electrodeposited Polymer Films with Both Superhydrophobicity and Superoleophilicity. *Phys. Chem. Chem. Phys.* **2008**, *10*, 4322–4326.

(58) Godeau, G.; Darmanin, T.; Guittard, F. Switchable Surfaces from Highly Hydrophobic to Highly Hydrophilic Using Covalent Imine Bonds. *J. Appl. Polym. Sci.* **2016**, *133*, 43130.

(59) Roquet, S.; Leriche, P.; Perepichka, I.; Jousselme, B.; Levillain, E.; Frère, P.; Roncali, J. 3,4-Phenylenedioxythiophene (PheDOT): a Novel Platform for the Synthesis of Planar Substituted π-Donor Conjugated Systems. *J. Mater. Chem.* **2004**, *14*, 1396–1400.

(60) Storsberg, J.; Schollmeyer, D.; Ritter, H. Route Towards New Heteroaromatic Benzo[1,4]dioxine Derivatives. *Chem. Lett.* **2003**, *32*, 140–141.

(61) Perepichka, I. F.; Roquet, S.; Leriche, P.; Raimundo, J.-M.; Frère, P.; Roncali, J. Electronic Properties and Reactivity of Short-Chain Oligomers of 3,4-Phenylenedioxythiophene (PheDOT). *Chem. Eur. J.* **2006**, *12*, 2960–2966.

(62) Grenier, C. R. G.; Pisula, W.; Joncheray, T. J.; Müllen, K.; Reynolds, J. R. Regiosymmetric Poly(dialkylphenylenedioxythiophene)s: Electron-Rich, Stackable p-Conjugated Nanoribbons. *Angew. Chem., Int. Ed.* **2007**, *46*, 714–717.

(63) Poverenov, E.; Sheynin, Y.; Zamoshchik, N.; Patra, A.; Leitus, G.; Perepichka, I. F.; Bendikov, M. Flat Conjugated Polymers Combining a Relatively Low HOMO Energy Level and Band Gap: Polyselenophenes Versus Polythiophenes. *J. Mater. Chem.* **2012**, *22*, 14645–14655.

(64) Krompiec, M. P.; Baxter, S. N.; Klimareva, E. L.; Yufit, D. S.; Congrave, D. G.; Britten, T. K.; Perepichka, I. F. 3,4-Phenylenedioxythiophenes (PheDOTs) Functionalized with Electron-Withdrawing Groups and Their Analogs for Organic Electronics. *J. Mater. Chem. C* **2018**, *6*, 3743–3756.

(65) Ponder Jr., J. F.; Schmatz, B.; Hernandez, J. L.; Reynolds, J. R. Soluble Phenylenedioxythiophene Copolymers via Direct (Hetero)Arylation Polymerization: a Revived Monomer for Organic Electronics. *J. Mater. Chem. C* **2018**, *6*, 1064–1070.

(66) Shibasaki, K.; Watanabe, M.; Kijima, M. Synthesis and Characterization of Soluble Poly(3,4-phenylenedioxythiophene). *Synth. Met.* **2015**, *205*, 18–22.

(67) Shibasaki, K.; Yasuda, T.; Kijima, M. Organic Photovoltaics Based on Poly(3,4-phenylenedioxy-2,5-thienylenevinylene)s. *Electrochemistry* **2017**, *85*, 241–244.

(68) Darmanin, T.; Laugier, J.-P.; Orange, F.; Guittard, F. Recent Advances in the Potential Applications of Bioinspired Superhydrophobic Materials. *J. Colloid Interface Sci.* **2016**, *466*, 413–424.

(69) Darmanin, T.; Guittard, F. A One-Step Electrodeposition of Homogeneous and Vertically Aligned Nanotubes with Parahydrophobic Properties (High Water Adhesion). *J. Mater. Chem. A* **2016**, *4*, 3197–3203.

(70) Szczepanski, C. R.; M'Jid, I.; Darmanin, T.; Godeau, G.; Guittard, F. A Template-Free Approach to Nanotube-Decorated Polymer Surfaces Using 3,4-Phenylenedioxythiophene (PhEDOT) Monomers. *J. Mater. Chem. A* **2016**, *4*, 17308–17323.

(71) Gbilimou, A.; Darmanin, T.; Godeau, G.; Guittard, F. A Templateless Electropolymerization Approach to Nanorings Using Substituted 3,4-Naphthalenedioxythiophene (NaPhDOT) Monomers. *ChemNanoMat* **2018**, *4*, 140–147.

(72) Darmanin, T.; Godeau, G.; Guittard, F.; Klimareva, E. L.; Schewtschenko, I.; Perepichka, I. F. A Templateless Electropolymerization Approach to Porous Hydrophobic Nanostructures Using 3,4-Phenylenedioxythiophene Monomers with Electron-Withdrawing Groups. *ChemNanoMat* **2018**, *4*, 656–662.

(73) Mee, S. P. H.; Lee, V.; Baldwin, J. E. Stille Coupling Made Easier—The Synergic Effect of Copper(I) Salts and the Fluoride Ion. *Angew. Chem. Int. Ed.* **2004**, *43*, 1132–1136.

(74) Bin, F.; Qu, L.; Shi, G. Electrochemical Polymerization of Anthracene in Boron Trifluoride Diethyl Etherate. *J. Electroanal. Chem.* **2005**, *575*, 287–292.

(75) Huang, Z.; Qu, L.; Shi, G.; Chen, F.; Hong, X. Electrochemical polymerization of naphthalene in the electrolyte of boron trifluoride diethyl etherate containing trifluoroacetic acid and polyethylene glycol oligomer. *J. Electroanal. Chem.* **2003**, *556*, 159–165.

(76) Zhu, G.; Xu, J.; Yue, R.; Lu, B.; Hou, J. Novel Poly-Bridged-Naphthalene with Blue-Light-Emitting Property via Electropolymerization. *J. Appl. Polym. Sci.* **2012**, *123*, 2706–2714.

(77) Hara, S.; Toshima, N. Electrochemical Polymerization of Aromatic Hydrocarbons on an ITO Electrode Using a Composite Electrolyte of Aluminum Chloride and Copper(I) chloride. *J. Eelectroanal. Chem.* **1994**, *379*, 181–190.

(78) Zhao, Y.; Stejskal, J.; Wang, J. Towards Directional Assembly of Hierarchical Structures: Aniline Oligomers as the Model Precursors. *Nanoscale* **2013**, *5*, 2620–2626.

(79) Poverenov, E.; Li, M.; Bitler, A.; Bendikov, M. Major Effect of Electropolymerization Solvent on Morphology and Electrochromic Properties of PEDOT Films, *Chem. Mater.* **2010**, *22*, 4019–4025.

(80) Krossing, I.; Raabe, I. Noncoordinating Anions – Fact or Fiction? A Survey of Likely Candidates. *Angew. Chem. Int. Ed.* **2004**, *43*, 2066–2090.

(81) Kim, J. T.; Seol, S. K.; Je, J. H.; Hwu, Y.; Margaritondo, G. The Microcontainer Shape in Electropolymerization on Bubbles. *Appl. Phys. Lett.* **2009**, *94*, 034103.

(82) McCarthy, C. P.; McGuinness, N. B.; Carolan, P. B.; Fox, C. M.; Alcock-Earley, B. E.; Breslin, C. B.; Rooney, A. D. Electrochemical Deposition of Hollow N-Substituted Polypyrrole Microtubes from an Acoustically Formed Emulsion. *Macromolecules* **2013**, *46*, 1008−1016.

(83) Sutton, S. J.; Vaughan, A. S. Morphology and Molecular Ordering in Films of Polypyrrole p-Toluene Sulfonate. *Polymer* **1996**, *37*, 5367–5374.

(84) Parakhonskiy, B.; Andreeva, D.; Möhwald, H.; Shchukin, D. G. Hollow Polypyrrole Containers with Regulated Uptake/Release Properties. *Langmuir* **2009**, *25*, 4780–4786.

(85) Parakhonskiy, B.; Shchukin, D. Polypyrrole Microcontainers: Electrochemical Synthesis and Characterization. *Langmuir* **2015**, *31*, 9214−9218.

(86) Thiam, E. h. Y.; Dramé, A.; Sow, S.; Sene, A.; Szczepanski, C. R.; Dieng, S. Y.; Guittard, F.; Darmanin, T. Designing Nanoporous Membranes through Templateless Electropolymerization of Thieno[3,4-b]thiophene Derivatives with High Water Content. *ACS Omega* **2019**, *4*, DOI: 10.1021/acsomega.9b00969.

(87) Sane, O.; Diouf, A.; Pan, M.; Cruz, G. M.; Savina, F.; Méallet-Renault, R.; Dieng, S. Y.; Amigoni, S.; Guittard, F.; Darmanin, T. Nanotubular Structures Through Templateless Electropolymerization using Thieno[3,4-b]thiophene Derivatives with Different Substituents and Water Content. *Electrochim. Acta* **2019**, *320*, 134594.

(88) Wenzel, R. N. Resistance of Solid Surfaces to Wetting by Water. *Ind. Eng. Chem.* **1936**, *28*, 988–994.

(89) Cassie, A.; Baxter, S. Wettability of Porous Surfaces. *Trans. Faraday Soc.* **1944**, *40*, 546–551.

GRAPHICAL ABSTRACT

Small changes in the side-chain environment of thiophene monomers lead to rich variations of the surface morphology of electrodeposited polymers including highly parahydrophobic nanostructures.

